

QUANTUM OTTO MACHINES POWERED BY A SINGLE QUBIT IN A SPIN STAR ENVIRONMENT

by

Majdi ALSULAMI^{a,*} and Eied Mahmoud KHALIL^{b,c}

^a Applied College in Alkamil, University of Jeddah, Jeddah, Saudi Arabia

^b Department of Mathematics, College of Science, Taif University, Taif, Saudi Arabia

^c Mathematics Department, Faculty of Science, Al-Azhar University, Cairo, Egypt

Original scientific paper

<https://doi.org/10.2298/TSCI2406867A>

This paper examines the performance analysis of quantum Otto machines (QOM) driven by a single qubit system embedded within a spin star environment. We investigate various thermodynamic correlations during the operation of these machines, including work performed, heat absorbed, and heat emissions. For the sake of simplicity, our exploration centers around two scenarios: one where the central qubit interacts with a single spin and another where it interacts with four qubits. Our findings reveal that QOM employing this system exhibit unique thermodynamic properties. Notably, we observe that the QOM can achieve enhanced levels of work performed as the number of spins in the environment increases. Furthermore, both the work performed and the efficiency of the QOM are influenced by the variation in detuning and coupling strength parameters across the four stages of its operation. Additionally, we demonstrate that careful selection of these parameters enables the optimization of QOM performance. In certain instances, the performance of the Otto cycle can be stabilized to emulate the behaviour of a heat engine by manipulating the coupling values while simultaneously controlling the frequency of the central qubit.

Key words: quantum Otto machines, spin star environment, work performed, thermodynamic correlations, quantum heat engines

Introduction

Quantum thermodynamics has emerged as one of the most dynamic and rapidly evolving fields in recent years. It builds upon the fundamental principles of classical thermodynamics, such as heat, work, and the laws of thermodynamics, but treats them in a quantum mechanical framework [1, 2]. By leveraging the classical physical content, quantum models of classical engines have been developed, such as the laser [3]. As the field continues to advance, the concepts of the Otto cycle [4, 5] and Carnot cycle [6, 7] have been exploited to design a wide variety of quantum heat engines [8]. In this context, a diverse range of quantum working materials have been utilized to create these engines, including qubits [9, 10], two-qubits [11-13], and photons [14], and harmonic oscillators [15]. Additionally, some work has addressed quantum engines that power multiple objects [16, 17]. Experimental laboratories have made significant progress in designing, estimating, and verifying these heat engines in practice [18]. Previous studies have performed fundamental analyses of the properties of quantum engines, particularly those related to work production and efficiency [19]. In recent years, some quan-

* Corresponding author, e-mail: mdalsolami@uj.edu.sa

tum heat engines have been designed under the assumption of Maxwell's demon, validating a series of quantum information theories and their applications to quantum heat engines [20]. The comparative between Otto and Carnot cycles in spin chain working fluid are introduced [21].

The study of quantum thermal machines has been significantly advanced by the concepts introduced in open quantum systems theory [22]. This theory provides a framework for measuring the evolution and simulating the interaction between the internal system and the external environment [23-25]. One of the most fundamental features that distinguish quantum systems from classical ones is quantum correlations [26-28]. These correlations are considered to be a key factor that determines the departure of quantum systems from the classical description of physical systems [29]. In particular, entanglement between parts of quantum systems has been extensively studied [30]. Quantum systems are being investigated as a major source of information processing, and quantum correlations have also been widely considered in the context of many-body systems [31] and more recently in quantum thermodynamics [32]. Quantum correlations have been shown to have a significant impact on the performance of quantum thermal machines. For example, they can enhance the efficiency of heat engines beyond the classical limit [6]. Additionally, they can be used to design quantum refrigerators that cool quantum systems to temperatures below the environment temperature [33].

In the present study, we employ a single qubit system in a spin star configuration as the working substance. The system comprises a single central qubit that interacts locally with each of the surrounding spins, while there is no internal or mutual interaction among the surrounding spins [34]. This model enables us to investigate the Otto cycle under varying conditions of atom numbers present in the interaction as the working substance of the machine. The primary objective of this research is to address the following questions: Does increasing the atom number enhance the work done and the efficiency of the machine? Does controlling the frequency of the central atom exert a significant impact on the machine's performance? What are the consequences of augmenting the coupling strength between the central atom and the surrounding environment? To this end, we delve into the investigation of this model with different atom numbers and varying coupling strengths to achieve optimal performance of the Otto cycle using this type of working substance. The study provides valuable insights into the behavior of the quantum Otto cycle in a spin star environment and the factors that influence its efficiency and work output. The motivation of this paper is to explore the performance of a quantum Otto cycle in a spin star environment using a single qubit system as the working substance. The study aims to address critical questions related to the effects of atom number, frequency control, and coupling strength on the machine's efficiency and work output.

Suggested working fluid

In this section, the physical Hamiltonian model of the working fluid of the QOC consists of a single qubit system with the frequency Ω surrounded by non-interacting N spin environment with the frequency ω . This working fluid can be expressed [34]:

$$H = \frac{\Omega}{2} \hat{\sigma}_z + \frac{\omega}{2} \sum_{k=1}^N \hat{S}_z^{(k)} + \lambda \left(\hat{\sigma}_+ \sum_{k=1}^N \hat{S}_-^{(k)} + \hat{\sigma}_- \sum_{k=1}^N \hat{S}_+^{(k)} \right) \quad (1)$$

where $\sigma_{z(\pm)}$ is the inversion (raising/lowering) Pauli matrix, while $\hat{S}_{z(\pm)}$ – the spin $-1/2$ inversion (raising/lowering) operator, and λ – the homogeneous coupling interaction between the center qubit and surrounding environment. If the surrounding bath rearranged as a single effective angular momentum quantum operator J , the Hamiltonian (1) can be re-written as a two-particle:

$$\mathcal{H} = \frac{\Omega}{2} \hat{\sigma}_z + \frac{\omega}{2} J_z + \lambda (\hat{\sigma}_+ J_- + \hat{\sigma}_- J_+) \quad (2)$$

here

$$\hat{J}_i = \sum_{k=1}^N \hat{S}_i^{(k)}$$

which operate on the state [35]:

$$\hat{J}_z |j, m\rangle = m |j, m\rangle \quad (3)$$

$$\hat{J}_+ |j, m\rangle = \sqrt{(j-m)(j+m+1)} |j, m+1\rangle \quad (4)$$

$$\hat{J}_- |j, m\rangle = \sqrt{(j-m+1)(j+m)} |j, m-1\rangle \quad (5)$$

where j is the half-integer number and $m = -j, -j+1, \dots, j-1, j$. These operators obey the commutation $[\hat{J}_z, \hat{J}_\pm] = \pm \hat{J}_\pm$. For N spin particle, we put $N = 2j$ and this allowed $m = -N/2, (-N/2) + 1$, and $N/2$. The eigenvalues of \mathcal{H} :

$$E_{1,2} = \omega \left(m + \frac{1}{2} \right) \pm \sqrt{\frac{\Delta^2}{4} + \lambda^2 (j-m)(j+m+1)} \quad (6)$$

where $\Delta = \Omega - \omega$. The corresponding eigenvectors:

$$|\psi\rangle_1 = \cos \frac{\theta}{2} |e, j, m\rangle + \sin \frac{\theta}{2} |g, j, m+1\rangle \quad (7)$$

$$|\psi\rangle_2 = -\sin \frac{\theta}{2} |e, j, m\rangle + \cos \frac{\theta}{2} |g, j, m+1\rangle$$

where

$$\tan \theta = \frac{2\lambda \sqrt{(j-m)(j+m+1)}}{\Delta} \quad (8)$$

We focus on the two cases $j = 1/2$ and $j = 2$. For $j = 0.5$, then $m = -1/2, 1/2$, and the eigenenergies can be given:

$$j = \frac{1}{2} \rightarrow \begin{cases} m = \frac{1}{2} \rightarrow \begin{cases} E_1 = \frac{|\Delta|}{2} + \omega \\ E_2 = -\frac{|\Delta|}{2} + \omega \end{cases} \\ m = -\frac{1}{2} \rightarrow \begin{cases} E_1 = \frac{1}{2} \sqrt{\Delta^2 + 4\lambda^2} \\ E_2 = \frac{-1}{2} \sqrt{\Delta^2 + 4\lambda^2} \end{cases} \end{cases} \quad (9)$$

Likewise, one can obtained the eigenenergies of $j = 2$, where we have ten eigenenergies in this case.

The adiabatic process, a crucial stage in a quantum Otto cycle, relies on the system's eigenenergies changing in a specific manner as the system parameters are altered. To ensure proper quantum behaviour, it is essential to investigate how the energy levels are affected by changes in the system parameters, avoiding level crossings. Figure 1 illustrates the energy levels of a quantum system at various values of j, λ , and Δ . The ground state and ex-cited state are

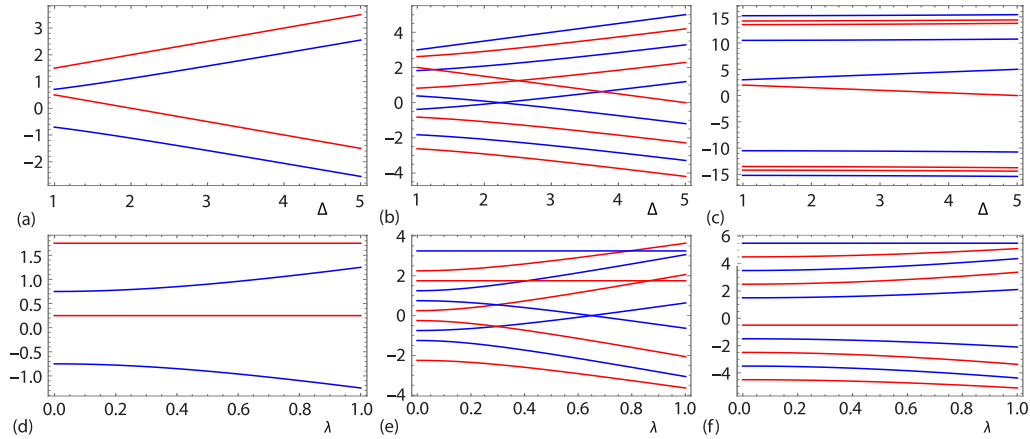


Figure 1. The upper row is energy levels as a function of Δ ; (a) $\lambda = 0.5\omega, j = 0.5$, (b) $\lambda = 0.5\omega, j = 2$, (c) $\lambda = 0.6\omega, j = 2$, the lower row is energy levels as a function of λ , (d) $\Delta = 1.5\omega, j = 0.5$, and (e) $\Delta = 1.5\omega, j = 2$, (f) $\Delta = 6\omega, j = 2$

initially separated by enhancing the coupling strength between the system and the surrounding medium at $j = 0.5$ (first column). Further increases in the detuning parameter, fig. 1(a), and coupling strength, fig. 1(d), widen the energy level separation. Notably, increasing the number of surrounding atoms ($j = 2$, four atoms) significantly and rapidly increases the energy level separation. However, the eigenenergies intersect at low coupling or detuning values, figure 1(b) and 1(e). As the detuning and coupling strength increase, the energy levels return to non-crossing. Increasing the coupling strength λ is necessary when the energy levels depend on the detuning, fig. 1(c). Moreover, if the energy levels are sensitive to the range of coupling strength allowed, fig. 1(f), we must increase the detuning parameter. As the detuning and coupling strength increase, the energy levels are significantly reordered, and the adiabatic process is better preserved. In-depth physical analysis displays that the preservation of the adiabatic process is closely related to the frequency strength of the central atom and its degree of coupling to the surrounding atoms. These parameters can be adjusted during device manufacturing to optimize the adiabatic process. To provide a more informative discussion, we will focus on the change in coupling strength and detuning in our studies, while keeping in mind the broader physical context.

Quantum Otto cycle

In accordance with the principles of thermodynamics, the expectation value of the working fluid (2) characterizes the internal energy of the QOC, specifically expressed:

$$U = \langle \mathcal{H} \rangle = \sum_i p_i(T) E_i$$

where $p_i(T)$ is the distributed probabilities determined by $p_i(T) = (1/Z)e^{-\beta E_i}$ where $Z = \sum_i e^{-\beta E_i}$ serves as the partition function, E_i – the eigenenergy levels inherent to the working fluid. It is notable that $\beta = 1/kT$, where $k = 1$, and T represents the temperature parameter in this context. As per the foundational principle of the First law of thermodynamics, the differential of internal energy, δU , can be separated into two distinct components: the transferred heat and the work done. This can be expressed mathematically [36]:

$$\delta U = \delta Q + \delta W = \sum_i E_i dp_i(T) + \sum_i p_i(T) dE_i \quad (10)$$

During the QOC, the working fluid underwent four stages, two adiabatic and two isochoric processes. We supposed that the parameters λ and Δ are changed during the cycle. The four stages are briefly expressed as:

Stage 1. Isochoric process, in this initial stage, the working fluid absorbs a certain amount of heat from the hot reservoir, resulting in an increase in the temperature of the working fluid to T_h . In this scenario, the probabilities distributed among the system vary in accordance with $p_i(T_h)$. However, no work is performed and the eigenenergy does not remain constant. The heat absorbed during this process can be calculated using:

$$Q_h = \sum_i E_i^h [p_i(T_h) - p_i(T_c)] \quad (11)$$

where E_i^h is the dependent on the hot parameters.

Stage 2. Adiabatic process, moving on the second stage, the working fluid is disconnected from the hot reservoir. Consequently, the eigenenergy E_i^h changed to E_i^c , and also the working fluid parameters are changed from T_h , λ_h , and Δ_h to T_c , λ_c , and Δ_c . During this stage, the distributed probabilities remain unaltered, while the work performed undergoes a change.

Stage 3. Isochoric process, in which the working fluid is connected to a cold reservoir at temperature T_c . The distributed probabilities are altered to $p_i(T_c)$, while there is no work performed, resulting in no change in the eigenenergy E_i^h . However, the heat released during this process can be given:

$$Q_c = \sum_i E_i^c [p_i(T_c) - p_i(T_h)] \quad (12)$$

Stage 4. Adiabatic process, this is the final process, where the working fluid is segregated from the cold reservoir and the parameters λ_c and Δ_c are reverted to their initial values λ_h and Δ_h . However, the work is done to return the energy to the system. From Stages 2 and 4, one can derive the work executed due to alterations in the control system parameters. The work performed in the QOC can be expressed:

$$\mathcal{W} = (E_i^h - E_i^c) [p_i(T_h) - p_i(T_c)] \quad (13)$$

The efficiency of a QHE can be expressed:

$$\varepsilon = \frac{\mathcal{W}}{Q_h} = 1 + \frac{Q_c}{Q_h} \quad (14)$$

Work extraction and efficiency

This section delves into the exploration of work extraction, anticipated heat machine, and efficiency concerning heat exchange.

Figure 2 represents the work performed by a quantum Otto machine for our hypothetical system when the central atom is coupled to either one other atom ($j = 0.5$) or four atoms ($j = 2$). The first row of the figure depicts the work as a function of the $(\Delta_h/\omega, \Delta_c/\omega)$ -plane with varying values of λ . At $j = 0.5$ and constant λ throughout the four stages with $\lambda_{h,c} = 0.5\omega$, it is evident that increasing Δ_c/ω results in negative work, while increasing Δ_h/ω enhances the values of positive work, refer to fig. 2(a). However, if $\lambda_h = 0.5\omega$, $\lambda_c = \omega$ varies across the four stages, as shown in fig. 2(b), increasing Δ_c/ω signifies more negative work, while the region where the work is positive expands without a substantial increase in the positive work. At $j = 2$ in fig. 2(c),

it becomes necessary to augment the values of $\lambda_{h,c} = 6\omega$ to preserve the adiabatic process, as discussed in fig. 1. Notably, both the negative and positive values of the work performed have increased significantly while maintaining the same behaviour due to the increments in $\Delta_{h,c}/\omega$. This observation suggests that Δ_c/ω and Δ_h/ω are invariably linked to the direction of work, implying that Δ_c/ω is associated with negative work, leading to energy loss or shrinkage of the system, thereby causing a decrease in its internal energy. Conversely, Δ_h/ω is associated with positive work, wherein the system gains energy or exerts force to expand its volume, resulting in an increase in its internal energy.

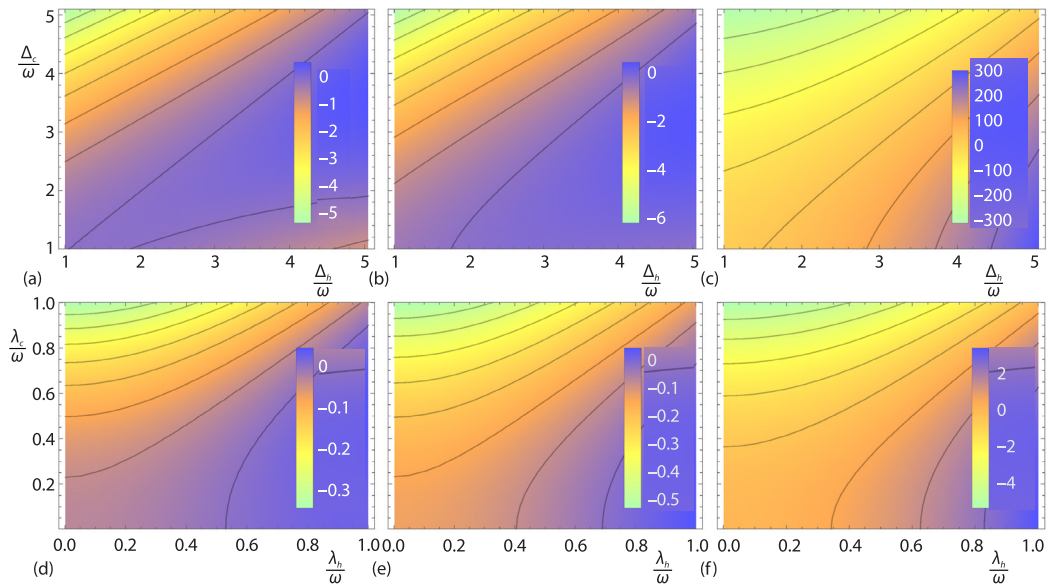


Figure 2. The upper row is work done as a function of Δ_h/ω and Δ_c/ω ; (a) $\lambda_h = \lambda_c = 0.5\omega$, (b) $\lambda_h = 0.5\omega$, $\lambda_c = \omega$, $j = 0.5$, (c) $\lambda_h = \lambda_c = 6\omega$, $j = 2$, the lower row is work done as a function of λ_h and λ_c , (d) $\Delta_h = \Delta_c = 1.5\omega$, $j = 0.5$, (e) $\Delta_h = 1.5\omega$, $\Delta_c = 2\omega$, $j = 0.5$, and (f) $\Delta_h = \Delta_c = 6\omega$, $j = 2$

The second row of fig. 2 illustrates the work performed in the $(\lambda_h/\omega, \lambda_c/\omega)$ -plane at varying values of $\Delta_{h,c}/\omega$. Figure 2(d) demonstrates that increasing λ_h/ω enhances the maximum values of the positive work done while increasing λ_c/ω amplifies the negativity of the work done, all at constant $\Delta_{h,c} = 1.5\omega$ throughout the four stages. By increasing $\Delta_c = 3\omega$ in comparison $\Delta_h = 1.5\omega$, the negative values of the work increase significantly more than those observed for the positive work, refer to fig. 2(e). Upon augmenting the number of atoms ($j = 2$) and maintaining a constant $\Delta_{h,c} = 6\omega$ with larger values (to preserve adiabaticity), the work becomes more pronounced, whether positive or negative. However, the positive work is confined only to the higher values of λ_h/ω .

From these observations, it can be inferred that the internal energy of the Otto machine decreases as a consequence of increasing λ_c/ω . In this scenario, thermal energy is transferred from the system to the atoms. Conversely, energy is transferred from the atoms to the system by increasing λ_h/ω . It is evident from this figure that $\lambda_{h,c}/\omega$ and $\lambda_{h,c}/\omega$ exert a similar influence on the work performed in raising or lowering the internal energy of an Otto cycle.

Let us now direct our attention the investigation of the efficiency of the Otto cycle through fig. 3, under the same conditions assumed in fig. 2. It is important to note that, in gen-

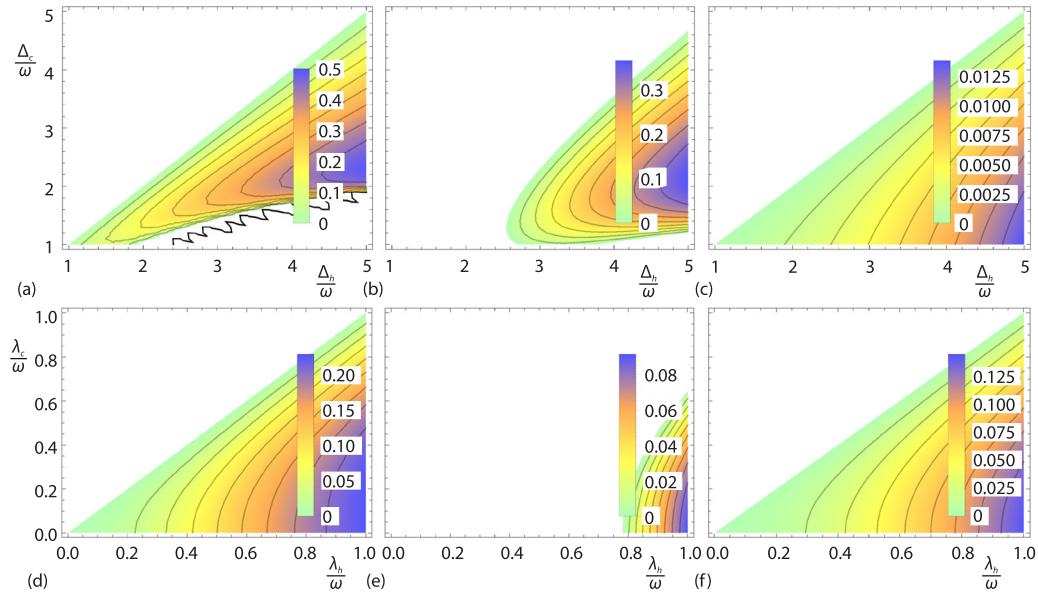


Figure 3. The efficiency function ε with the same parameters that displayed in fig. 2

eral, the white area represents negative efficiency, which does not correspond to a quantum heat engine (QHE). Therefore, we have disregarded its analysis in this context. In the $\Delta_h/\omega - \Delta_c/\omega$ -plane, figs. 3(a)-3(c), it is evident that the Otto cycle exhibits an increasing efficiency that is directly proportional to the increase in Δ_h/ω . Maintaining the coupling ($\lambda_h = \lambda_c = 0.5\omega$) constant during the four stages results in the efficiency dividing the plane almost evenly. However, with increasing Δ_h/ω in the case of one atom and small values of Δ_c/ω , the efficiency diminishes once again, fig. 3(a). Nevertheless, varying $\lambda_h = 0.5\omega$, $\lambda_c = \omega$ during the cycle serves to render the efficiency of the QHE non-symmetric, and its maximum value decreases even with increasing Δ_h/ω . As a consequence of increasing the number of atoms ($j = 2$), the efficiency of the QHE decreases significantly, nearly reaching zero. In comparison the case of one atom, the efficiency of Otto approaches the efficiency of a Carnot machine in certain regions, where:

$$\varepsilon = \varepsilon_C = 1 - \frac{T_c}{T_h} = 0.5$$

On the other hand, the efficiency increases in the $(\lambda_h/\omega - \lambda_c/\omega)$ plane, figs. 3(d)-3(f), due to increasing λ_h/ω while decreasing with increasing λ_c/ω . The efficiency divides this plane evenly when both Δ_h/ω and Δ_c/ω are equal, while their asymmetry reduces efficiency and induces asymmetry. In this plane, the efficiency does not attain the Carnot efficiency, and augmenting the number of surrounding atoms marginally reduces the efficiency.

We now embark on an investigation into the impact of varying $\Delta_{h,c}$ and $\lambda_{h,c}$ on the Otto cycle and the resultant machines when $j = 0.5$. To this end, we plot the work performed (curve – 1), the energy emitted (curve – 2), the energy absorbed (curve – 3), and the efficiency (curve – 4). In the first scenario, the four quantum parameters are functions of Δ_h/ω when $\Delta_c = 1.5\omega$. Consequently, the machine resulting from the cycle is contingent upon the changes in λ_h/ω and λ_c/ω . The QOM displays four operations as a results of change working fluid parameters, which are:

- Quantum heat engine (QHE): $\mathcal{W} > 0$, $Q_h > 0$, and $Q_c < 0$
- Refrigerator: $\mathcal{W} < 0$, $Q_h < 0$, and $Q_c > 0$
- Accelerator: $\mathcal{W} < 0$, $Q_h > 0$, and $Q_c < 0$
- Heater: $\mathcal{W} < 0$, $Q_h < 0$, and $Q_c < 0$

Figure 4(a) illustrates that in the case of constant $\lambda_h = \lambda_c = 0.5\omega$, the resulting machine initially operates as an accelerator, followed directly by a QHE, then a heater, and subsequently the cycle reverts to an accelerator again during the evolution of Δ_h/ω . However, when $\lambda_c > \lambda_h$, we observe from fig. 4(b) that the thermal processes expand, resulting in the emergence of an accelerator initially, followed by a QHE, and then an accelerator once more. Figure 4(c) presents a distinct behaviour when $\lambda_c < \lambda_h$. In this case, the Otto cycle initially exhibits a QHE, which subsequently transforms into a heater and then into a quantum refrigerator. Throughout the aforementioned three cases, it is noteworthy that the efficiency of the resulting thermal machine, in terms of maximum values, is superior in the scenario where $\lambda_c < \lambda_h$. However, the duration of the cycle is longer in the case where $\lambda_c > \lambda_h$.

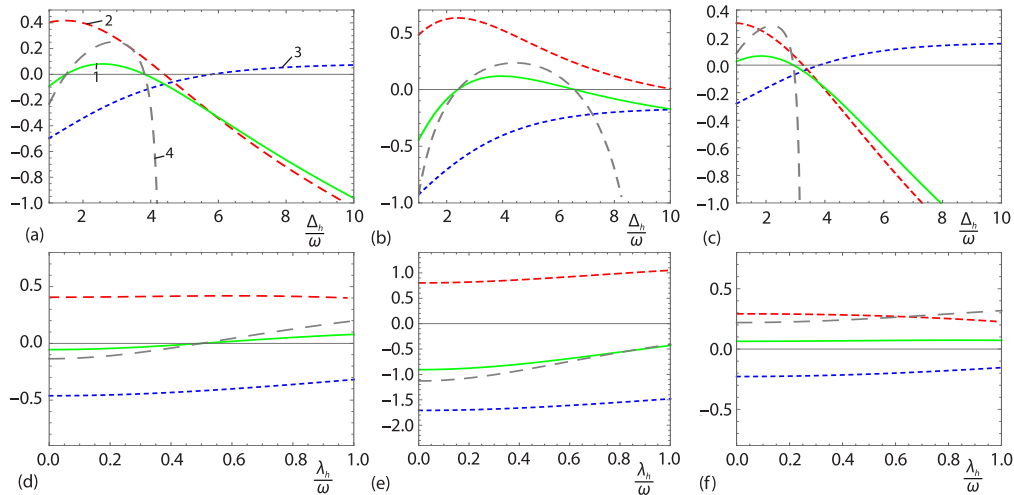


Figure 4. The competitive between work done \mathcal{W} , heat released Q_c , heat absorbed Q_h , and the efficiency ε for $j = 0.5$, the upper row the three function as a function of Δ_h/ω with $\Delta_c = 1.5\omega$; (a) $\lambda_h = \lambda_c = 0.5\omega$, (b) $\lambda_h = 0.1\omega$, $\lambda_c = 0.9\omega$, (c) $\lambda_h = 0.9\omega$, $\lambda_c = 0.1\omega$, the lower row the three function as a function of λ_h/ω with $\lambda_c = 0.5\omega$, (d) $\Delta_h = \Delta_c = 1.5\omega$, (e) $\Delta_h = 1.5\omega$, $\Delta_c = 3\omega$, and (f) $\Delta_h = 3\omega$, $\Delta_c = 1.5\omega$

In the second scenario, we depict the four quantifiers as a function of λ_h/ω when $\lambda_c = 0.5\omega$. It becomes evident that when $\Delta_h = \Delta_c = 1.5\omega$, the Otto cycle transitions from a thermal accelerator to a QHE at $\lambda_h = 0.5\omega$. This implies that when λ_h/ω is greater than λ_c/ω , the resulting machine operates as a QHE with a constant efficiency. The Δ also exerts a significant influence. If Δ_h/ω is less than Δ_c/ω , the resulting machine manifests as an accelerator with quasi-stable behaviour. On the other hand, if Δ_h/ω is greater than Δ_c/ω , the resulting machine operates as a QHE. It is evident that fixing the values of during the period (during the period in which the adiabatic process was preserved) is crucial for obtaining a more stable quantum machine, thereby preventing the undesirable switching between different types of machines.

Conclusions

In this study, we explored the QOM using a single qubit system in a spin star environment as the working substance, assuming that the central qubit interacts with one or four surrounding spins. We examined how to preserve the adiabatic process by preventing the crossing of energy levels of the two studied states. We presented an overview of the QOM, highlighting the changes in detuning parameter and coupling constant during the four stages. We investigated the work done, efficiency, absorbed heat, and emitted heat as a function of the detuning and coupling constants.

Our primary findings are summarized as follows.

- The number of surrounding spins significantly influences the Otto cycle's performance. Increasing the number of spins enhances the work done and the machine's efficiency. This is because a larger number of spins provides more potential energy levels for the system to transition between, leading to more work being done.
- The frequency of the central atom significantly impacts the machine's performance. Controlling the frequency of the central atom can improve the machine's efficiency. This is because the frequency of the central atom determines the energy difference between the two energy levels of the system, which can affect the machine's efficiency.
- The coupling strength between the central atom and the surrounding environment significantly impacts the machine's performance. Increasing the coupling strength can improve the machine's efficiency. This is because the coupling strength determines the rate at which the system can exchange energy with the environment, affecting the machine's efficiency.
- Changes in the central atom's frequency or coupling strength can generate different quantum machines. These machines can be controlled more effectively by regulating the coupling strength in the hot or cold bath. If the coupling strength is greater in the hot bath, we obtain a quantum thermal machine with constant performance at different detuning values.

In conclusion, our results suggest that the following strategies could be employed to enhance the performance of quantum Otto cycles using spin star environments. Utilize a system with a large number of surrounding spins to increase the work done and the machine's efficiency. Control the frequency of the central atom to improve the machine's efficiency. Increase the coupling strength between the central atom and the surrounding environment to improve the machine's efficiency.

Acknowledgment

This work was funded by the University of Jeddah, Jeddah, Saudi Arabia, under Grant No. (UJ-23-DR-213). Therefore, the authors thank the University of Jeddah for its technical and financial support.

References

- [1] Kosloff, R., Quantum Thermodynamics: A dynamical Viewpoint, *Entropy*, 15 (2013), 6, pp. 2100-2128
- [2] Millen, J., Xuereb, A., Perspective on Quantum Thermodynamics, *New J. Phys.*, 18 (2016), 011002
- [3] Scovil, H. E. D., Schulz-DuBois, E. O., Laser Cooling by Spontaneous Anti-Stokes Scattering, *Phys. Rev. Lett.* 2 (2959), 6, pp. 262-263
- [4] Kosloff, R., Rezek, Y., The Quantum Harmonic Otto Cycle, *Entropy*, 19 (2017), 4, 136
- [5] Altintas, F., Mustecaplioglu, O. E., General Formalism of Local Thermodynamics with an Example: Quantum Otto Engine with a Spin-1/2 Coupled to an Arbitrary Spin, *Phys. Rev. E*, 92 (2015), 2, 022142
- [6] Scully, M. O., *et al.*, Extracting Work From a Single Heat Bath Via Vanishing Quantum Coherence, *Science*, 299 (2003), 5608, pp. 862-864
- [7] Turkpence, D., *et al.*, A Photonic Carnot Engine Powered by a Spin-Star Network, *Europhys. Lett.*, 1175 (2017), 5, 50002.

- [8] Quan, H.-T., et al., Quantum Thermodynamic Cycles and Quantum Heat Engines, *Phys. Rev. E*, 76 (2007), 3, 031105
- [9] Brunner, N., et al., Entanglement Enhances Cooling in Microscopic Quantum Refrigerators, *Phys. Rev. E*, 89 (2014), 3, 032115
- [10] Campisi, M., et al., Non-Equilibrium Fluctuations in Quantum Heat Engines: Theory, Example, and Possible Solid State Experiments, *New J. Phys.*, 17 (2015), 3, 035012
- [11] Silva, R., et al., Performance of Autonomous Quantum Thermal Machines: Hilbert space Dimension as a Thermodynamical Resource, *Phys. Rev. E*, 94 (2016), 3, 032120
- [12] Niedenzu, W., et al., Performance Limits of Multilevel and Multipartite Quantum Heat Machines, *Phys. Rev. E*, 92 (2015), 4, 042123
- [13] Gardas, B., Deffner, S., Thermodynamic Universality of Quantum Carnot Engines, *Phys. Rev. E*, 92 (2015), 4, 042126
- [14] Dillenschneider, R., Lutz, E., Energetics of Quantum Correlations, *Europhys. Lett.*, 88 (2009), 5, 50003
- [15] Scopa, S., et al., Exact Solution of Time-Dependent Lindblad Equations with Closed Algebras, *Phys. Rev. A*, 99 (2019), 2, 022105
- [16] Campisi, M., Fazio, R., The Power of a Critical Heat Engine, *Nature Commun.*, 7 (2016), 1, 11895
- [17] Jaramillo, J., et al., Quantum Supremacy of Many-Particle Thermal Machines, *New J. Phys.*, 18 (2016), 7, 075019
- [18] Rosnagel, J. et al., A Single-Atom Heat Engine, *Science*, 352 (2016), 6283, pp. 325-329
- [19] Chatterjee, S., et al., Temperature-Dependent Maximization of Work and Efficiency in a Degeneracy-Assisted Quantum Stirling Heat Engine, *Phys. Rev. E*, 103 (2021), 6, 062109
- [20] Beyer, K., et al., Steering Heat Engines: A Truly Quantum Maxwell Demon, *Phys. Rev. Lett.*, 123 (2019), 25, 250606
- [21] Abd-Rabbou, et al., Comparative Study of Quantum Otto and Carnot Engines Powered by a Spin Working Substance, *Phys. Rev. E*, 108 (2023), 3, 034106
- [22] Breuer, H.-P., Petruccione, F., *The Theory of Open Quantum Systems*, Oxford University Press, New York, USA, 2002
- [23] Alotaibi, M. F., et al., Dynamics of an Atomic System Associated with A Cavity-Optomechanical System, *Res. Phys.*, 37, (2022), 105540
- [24] Khalil, E. M., Abd-Rabbou, M. Y., Robustness of a teleported State Influenced by Dipole Interaction and Magnetic Field under Intrinsic Decoherence, *Optik*, 267 (2022), 169703
- [25] Alruqi, A. B., et al., Visualization of the Interaction Dynamics between a Two-Level Atom and a Graphene Sheet Covered by a Laser Field, *Alex. Eng. J.*, 77 (2023), Aug., pp. 309-317
- [26] Alipour, S. B., et al., Correlations in Quantum Thermodynamics: Heat, Work, and Entropy Production, *Sci. Rep.*, 6 (2016), 1, 35568
- [27] Abd-Rabbou, M. Y., et al., Noise-Based Damping of Chaotic Entanglement in Pulsed Driven Two-Qubit System, *Ann. der Phys.*, 536 (2023), 3, 2300423
- [28] Abo-Kahla, D. A. M., et al., The Orthogonality Speed Of Two-Qubit State Interacts Locally with Spin Chain in the Presence of Dzyaloshinsky-Moriya Interaction, *Laser Phys. Lett.*, 18 (2021), 4, 045203
- [29] Modi, K., et al., The Classical-Quantum Boundary for Correlations: Discord and Related Measures, *Rev. Mod. Phys.*, 84 (2012), 4, pp. 1655-1707
- [30] Horodecki, R., et al., Quantum Entanglement, *Rev. Mod. Phys.*, 81 (2009), 2, 865
- [31] De Chiara, Sanpera, A., Genuine Quantum Correlations in Quantum Many-Body Systems: A Review of Recent Progress, *Rep. Prog. Phys.*, 81 (2018), 7, 074002
- [32] Goold, J. H., et al., The Role Of Quantum Information In Thermodynamics Topical Review, *J. Phys. A Math. Theor.*, 49 (2016), 143001
- [33] Tan, K. Y., et al., Quantum-Circuit Refrigerator, *Nature Commun.*, 8 (2017), 1, 15189
- [34] Hutton, A., Bose, S., Mediated Entanglement and Correlations in a Star Network of Interacting Spins, *Phys. Rev. A*, 69 (2004), 4, 042312
- [35] Abdalla, M. S., et al., Some Statistical Properties of the Interaction Between a Two-Level Atom and Three Field Modes, *Laser Phys.*, 25 (2015), 6, 065204
- [36] Quan, H. T., et al., Quantum Thermodynamic Cycles And Quantum Heat Engines, *Phys. Rev. E*, 76 (2007), 3, 031105